Journal Pre-proof

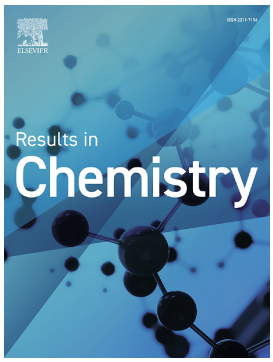

The impact of incorporating functional groups into MIL-101(Cr) for the removal of naproxen from aqueous solutions: A molecular dynamics study

A. Mohmmad, M.T. Hamed Mosavian, F. Moosavi

PII: S2211-7156(25)00476-X

DOI: https://doi.org/10.1016/j.rechem.2025.102493

Reference: RECHEM 102493

To appear in: *Results in Chemistry*

Received date: 24 September 2024

Accepted date: 3 July 2025

Please cite this article as: A. Mohmmad, M.T.H. Mosavian and F. Moosavi, The impact of incorporating functional groups into MIL-101(Cr) for the removal of naproxen from aqueous solutions: A molecular dynamics study, *Results in Chemistry* (2024), https://doi.org/10.1016/j.rechem.2025.102493

This is a PDF file of an article that has undergone enhancements after acceptance, such as the addition of a cover page and metadata, and formatting for readability, but it is not yet the definitive version of record. This version will undergo additional copyediting, typesetting and review before it is published in its final form, but we are providing this version to give early visibility of the article. Please note that, during the production process, errors may be discovered which could affect the content, and all legal disclaimers that apply to the journal pertain.

© 2025 Published by Elsevier B.V.

Journal Pre-proof

The impact of incorporating functional groups into MIL-101(Cr) for the removal of naproxen from aqueous solutions: A molecular dynamics study

A. Mohmmad[*], M.T. Hamed Mosavian[*^], F. Moosavi [**]

[*] Department of Chemical Engineering, Faculty of Engineering, Ferdowsi University of Mashhad, Iran. (E-mail: areej.mohmmad@mail.um.ac.ir ; mosavian@um.ac.ir).

[**] Department of Chemistry, Faculty of Science, Ferdowsi University of Mashhad, Iran. (E-mail: moosavibaigi@um.ac.ir).

^ Corresponding author: E-mail: mosavian@um.ac.ir .

Journal Pre-proof

Abstract

Water pollution with pharmaceutical compounds is one of the most dangerous problems, especially those that are used widely. Naproxen is used as an antipyretic, analgesic, and anti-inflammatory agent. With the discovery of Naproxen in drinking water in many countries, it has become a serious environmental risk. Therefore, a study on the potential of removing Naproxen from aqueous solutions using metal-organic frameworks MIL-101(Cr) through molecular dynamics simulation was conducted. The impact of functionalization the MIL-101(Cr) structure (OH, F, NH_2, and SO_3) on the diffusion coefficient and adsorption of Naproxen was also examined. Simulation results demonstrate that MIL-101(Cr)-SO_3, in addition to being environmentally friendly, achieves high efficiency in removing Naproxen molecules from aqueous solutions. The adsorption capacity of NAP on the MIL-101(Cr)-SO_3 is 590.45 mg/g, with an interaction energy between MIL-101(Cr)-SO_3 and NAP o -11044.35 kcal/mol. Therefore, MIL-101(Cr) can be proposed as a promising adsorbent for removing various pollutants from aqueous solutions.

Keywords: Adsorption; Metal-Organic Framework; MIL-101(Cr); Molecular Dynamics; Naproxen.

1. Introduction

Non-steroidal anti-inflammatory drugs (NSAIDs) consist of a large class of drugs with diverse functions and complex structures. They are generally weak organic aromatic acids, commonly used to treat patients suffering from pain and inflammatory conditions such as osteoarthritis, chronic pain, postoperative surgical conditions, and rheumatoid arthritis. Additionally, they are widely used as antipyretics and analgesics [1, 2]. NSAIDs can enter the environment and pollute it directly through pharmaceutical industries' wastewater or sewage, solid waste management plants, leachate from landfills, and hospital wastewater treatment plants [3]. They have high stability and reactivity, making them resistant to eco-toxicity and biodegradation posing a threat to the environment [4].

Naproxen (NAP), an anti-inflammatory drug, relieves mild to moderate pain from various causes, reduces joint stiffness, swelling, and pain associated with osteoarthritis [5]. Naproxen is prevalent due to its low human metabolic capability, widespread use, and poor degradation in wastewater treatment plants [6]. It has been detected at concentrations of 10 ng/L in natural water bodies and from 100 ng/L to several μg/L in wastewater, especially hospital wastewater [7]. Concerns have been raised about the adverse effects of NAP on aquatic life, such as its toxicity to fish and algae, as well as its potential side effects on humans [8]. Studies have shown that NAP not only affects the biological system in water bodies and the quality of water and living organisms, but also causes endocrine disruption and heart disease [9]. Therefore, it is imperative to find practical and effective methods for removing NAP from water and wastewater.

Adsorption technology plays a significant role in surface chemistry, primarily in the storage and separation of gases. It is also utilized for removing inorganic and organic pollutants from wastewater, as well as for the recovery and removal of heterogeneous catalysis and solvents [10]. Adsorption is considered one of the most promising and widely used technologies in wastewater treatment processes due to its safety, ease of use, high efficiency, and low cost [11, 12]. Various adsorbents such as activated carbon [13, 14], pure boron nitride [15], mesoporous carbons [16], zeolite-rich composites [17], and biochars [18] have been employed in the adsorption of NAP from aqueous solutions.

Metal-organic frameworks (MOFs) are porous inorganic-organic hybrid compounds. The structure of MOFs consists of a metal center and organic linkers [19, 20]. MOFs have distinctive properties

that make them efficient in water treatment processes[21-24], such as a large pore size and surface area, providing high adsorption capabilities for pollutants. Besides, most MOFs are stable in aqueous solutions and have active adsorption sites [20, 25]. MOFs can be manufactured on a large scale and designed to allow the adsorption or selective stimulation of pollutants. They can be formed in different shapes such as membranes, monoliths, pellets, or columns making them suitable for devices used in water treatment processes [25]. Among the well-known MOF nanocrystals, MIL-101(Cr) is recognized as a very stable 3D nanomaterial. It has terminal water molecules linked to Cr_3O building units. Removal of water under high vacuum leaves behind the chromium atoms, which serve as potential sites for a Lewis acid. It has been reported that Cr-MOFs offer strong stability in the water, base, and acid due to the strong metal-oxygen (Cr-O) bonds [26, 27]. MIL-101(Cr) is used for the adsorptive removal of various toxic organics from water and wastewater, such as bisphenol-A, Ketoprofen, Naproxen [28], sulfamethoxazole [29], methyl orange, Congo red [30], hexavalent chromium [31], bisphenol S [29], Pharmaceutical contaminants[32], dye [27], and clofibric acid [33]. Because MOFs have a benzene ring or an imidazole group in their structures, strong interaction with NAP and MOFs could be expected by forming a л-л stacking [34]. Several MOFs' including Fe_3O_4–FeBTC MOF [35], UIO-66-NH_2-Mlm [36], MIL-53 (Al) [37], MIL-101(Fe) [38], and UiO-66s [39], have been applied for the adsorption of NAP from aqueous solutions. However, none of them consider the role of functional group in the adsorption. It seems that the presence of different functional groups in MOF structures enhances the attraction between the adsorbate and the MOF [34]. It is clear that dynamic simulation is a valuable tool for researchers and professionals a like [21, 40-45], this study applies molecular dynamics (MD) simulation to explore and study the adsorption properties of NAP molecules in MIL-101(Cr)-X (X=OH, F, NH_2, and SO_3) structures at ambient pressure and temperature. Properties such as diffusion coefficient, adsorption energy, and fractional free volume are investigated to examine the most suitable MIL-101(Cr) for NAP capturing. Mean square displacement and radial distribution function evaluate the dynamics and pair correlations between the NAP molecules and the MOF structures.

Journal Pre-proof

2. Simulation Method

2.1. Model construction

In this research, Materials Studio package 2020 was utilized to study the adsorption of NAP molecules on the MIL-101(Cr)-X (X=OH, F, NH_2, SO_3). The structure of the NAP molecule was obtained from PubChem, while the structure of MIL-101(Cr) was downloaded using the atomic coordinates available in the Cambridge Structural Database (CSD) [46]. The MIL-(Cr)-OH unit cell was obtained by using the "Rebuild Crystals" module, selecting the P1 type group without changing cell dimensions. This unit cell was gone out the crystal state using the "Unbuild Crystal" module. Double and partial double bonds were then added to the new structure (Fig. 1a). The three-dimensional cubic cell of MIL-101(Cr)-OH was created using the "Build Crystals" module and the 227 FD-3M group. The dimensions of the MIL-101(Cr)-OH cell are 88.86Å×88.86Å×88.86Å (Fig. 1b). This cubic cell was simplified to a primitive unit cell using symmetry module. The volume of the primitive cell is only one-fourth of the original cubic cell volume (Fig. 1c). The primitive cell describes the MOF structure well and simultaneously decreases the computational requirements [47]. Hydrogen atoms were then added to the aromatic rings to achieve chemical equivalence.

To build MIL-101(Cr)-F, MIL-101(Cr)-NH_2 and MIL-101(Cr)-SO_3 structures, we started from the unit cell (Fig 1a). To obtain the MIL-101(Cr)-F structure, one oxygen atom in each Cr_3O group was replaced by one fluorine atom so the ratio of fluorine atoms to chromium atoms is 1:3.5. For the construction of the MIL-101(Cr)-NH_2 structure, at most one hydrogen atom in each organic ligand was replaced by an amine group, so the ratio of N:C is 1:8.5. To build the MIL-101(Cr)-SO_3 structure, the active amine group and fluorine atoms in the MIL-101(Cr)-NH_2 unit cell were replaced by the SO_3 group and oxygen atoms, respectively. The chemical composition, surface area, fractional free volume (FFV), and density of each MIL-101-X MOF are detailed in Table 1. The framework free volume decreases upon functionalization, while the density increases that is in acceptable accordance with literature [48]. From the other side of view, the obtained MIL-101(Cr) density is in good agreement Koroglu et al. study [49]. Figure 2 shows the MIL-101(Cr)-X structures after geometrical optimization.

2.2. Force field

The force field is applied to accurately compute the results consistent with experimental data. Additionally, it should be able to calculate all necessary particle interaction energies within the system while reducing computational time by focusing on essential interactions and disregarding weak ones between atoms [39]. Here, Universal Force Field (UFF) models the dispersion interactions of the MOF atoms. Acording to the literature, different molecular simulation studies have demonstrated that the UFF is appropriate for MOF structures and can reliably predict the diffusion and adsorption of molecules in different MOFs [12, 40].

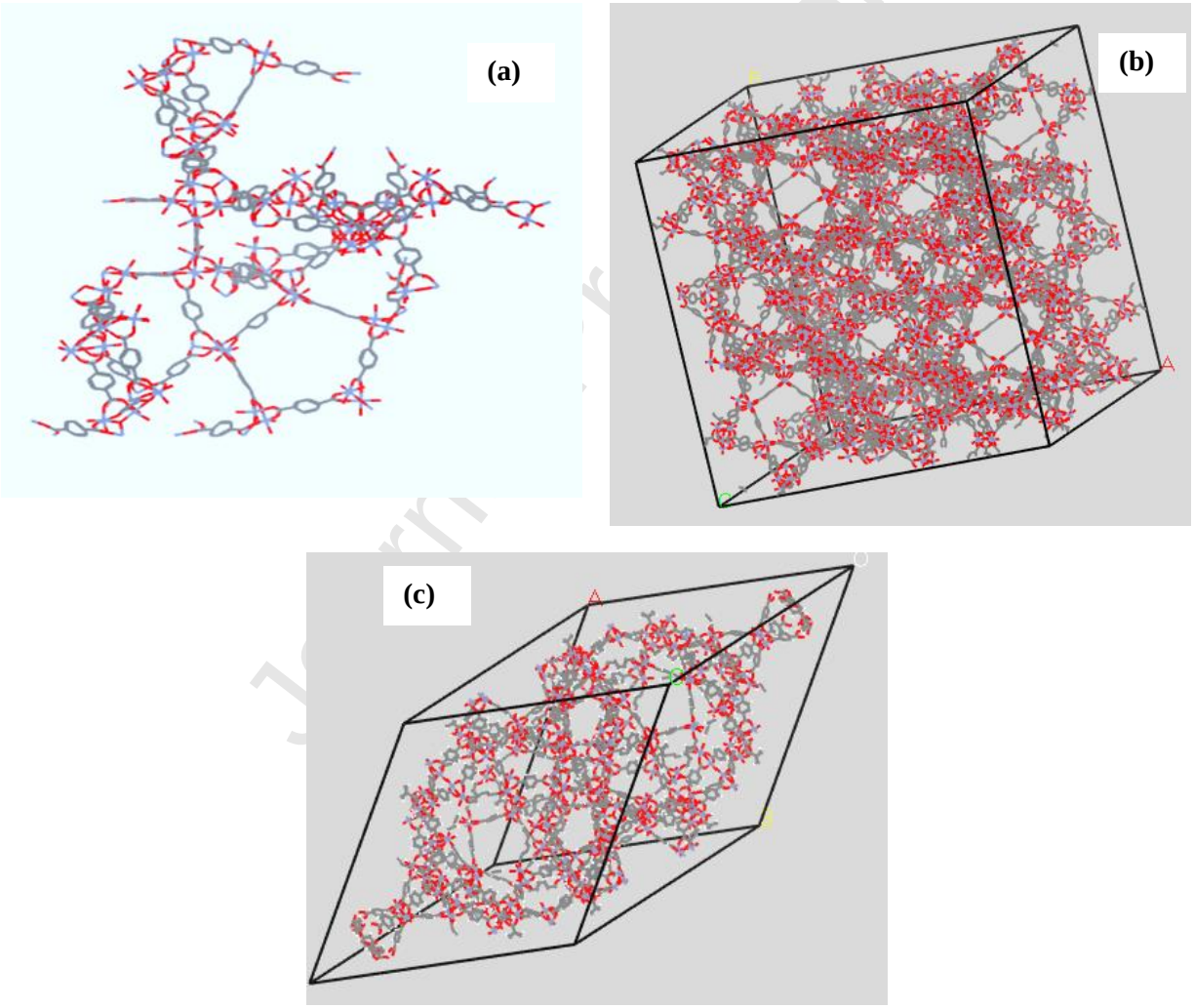

Figure 1: (a): The unit cell of MIL-101(Cr), (b): The cubic cell of MIL-101(Cr), (c): The primitive cell of MIL-101(Cr)

Table 1: Structural characteristics of the unit cells of the MIL structures

MOF	MOF Composition	M.W. (g/mol)	Density (g/cm^3)	Surface area ($Å^2$)	FFV %
MIL-101(Cr)-OH	$C_{1632}H_{1020}O_{1088}Cr_{204}$	48623.40	0.4595	31641.9	82.26
MIL-101(Cr)-F	$C_{1632}H_{912}O_{1028}F_{60}Cr_{204}$	48695.40	0.4576	31482.9	82.50
MIL-101(Cr)-NH_2	$C_{1632}H_{1056}N_{96}O_{1028}F_{60}Cr_{204}$	50183.40	0.4872	32474.9	81.29
MIL-101(Cr)-SO_3	$C_{1632}H_{912}O_{1376}S_{96}Cr_{204}$	56198.28	0.5309	35309.2	80.05

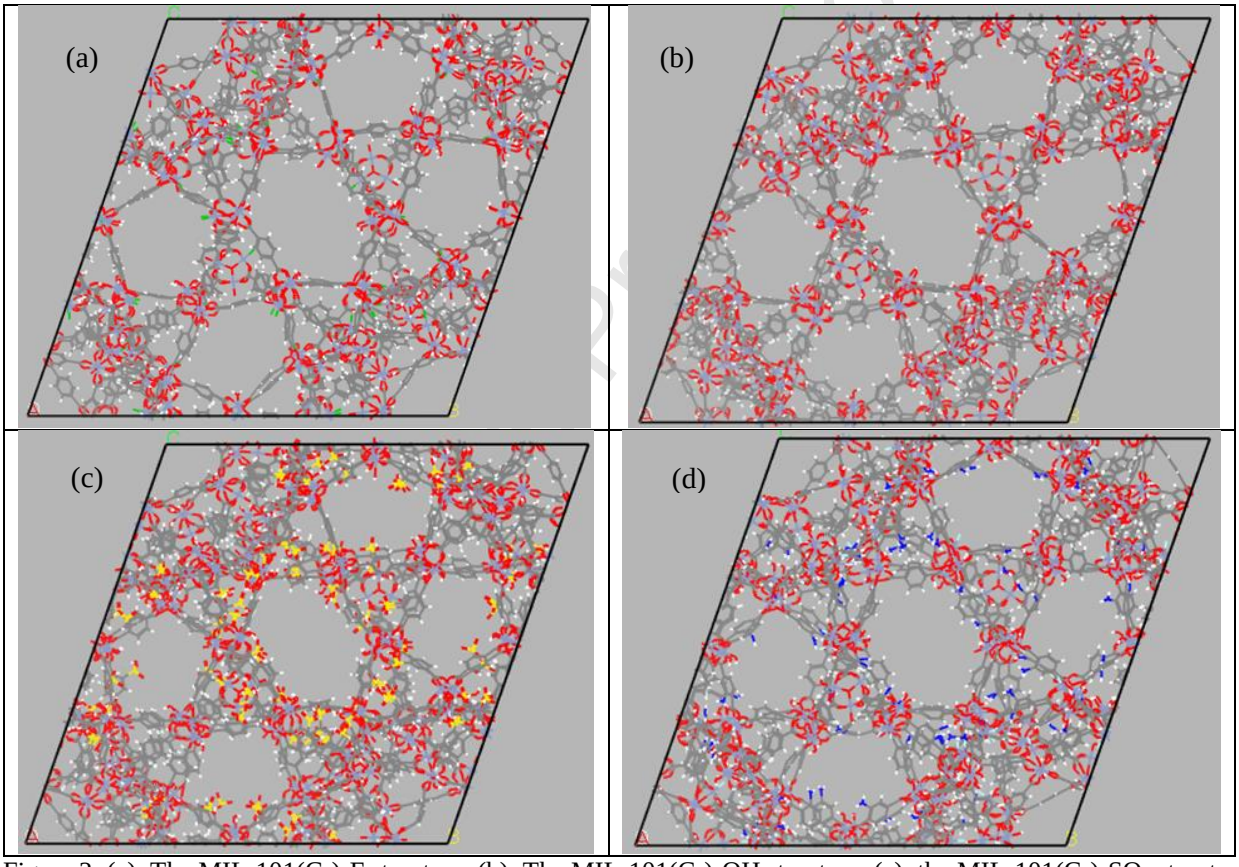

Figure 2: (a): The MIL-101(Cr)-F structure, (b): The MIL-101(Cr)-OH structure, (c): the MIL-101(Cr)-SO_3 structure and (d): the MIL-101(Cr)-NH_2 structure.

2.3. Box simulation

To study the transport and diffusion of NAP molecules in the MIL-101(Cr) structures, the MIL-101(Cr) structure is fixed at the center of the simulation cell (Fig.3). On one side, NAP and water

molecules are positioned, while vacuum is on the other side. The dimensions of the simulation box are 62.31 Å × 62.31 Å × 112.31 Å . During full MD simulations, the MIL-101 considered to be fixed while NAP and water molecules were flexible. Geometric optimization was carried out using the steepest descent algorithm for 2000 steps, followed by 5000 steps of the smart algorithm (a combination of quasi-Newton and steepest descent), and then an additional 7000 steps of the smart algorithm. The convergence criteria for force is 0.5 kcal/(mol.Å) and for energy is 0.001 kcal/mol. In this study, the QEq charge equilibration model was used to calculate the particl atomic charges of MIL-101 (Cr)-X [49]. The system was then equilibrated using an isochoric-isothermal ensemble (NVT) in a 5 ns MD simulation. A Nose thermostat was utillized to maintain the temperature at 298 K with a Q ratio of 0.01. Subsequently, 10 ns MD runs were conducted using a microcanonical ensemble (NVE) to obtain dynamic properties with a time step of 1 fs. The Ewald summation was employed to consider electrostatic interactions [50] with a buffer width of 0.5 Å and an accuracy of 0.001 kcal/mol. Van der Waals interactions were calculated using the atomic base method [50] with a cut-off distance of 30 Å. Long-range corrections were also considered during the optimization steps. Monte Carlo was used to obtain the surface adsorption characteristics (adsorption isotherm and adsorption energy). In the sorption module, the adsorption isotherm task and Metropolis method in the range of 10 to 1000 kPa were used to obtain the results.

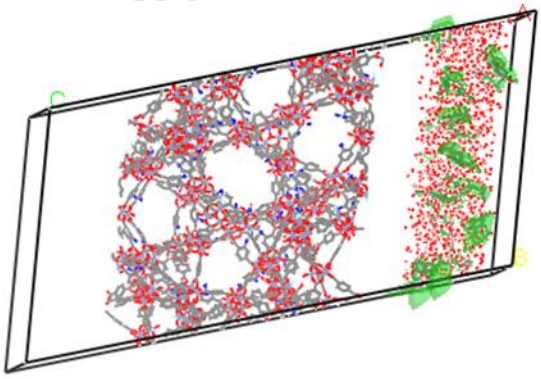

Figure 3: The initial simulation cell.

2.4. Computational procedures

Adsorption energy, also known as interaction energy, is the energy released when one mole of inhibitor (adsorbate) molecules is adsorbed on the surface of the adsorbent. In this MD simulation

study, the interaction energy between NAP molecules and the MIL-101(Cr) framework structures was calculated using the following relation [44]:

$$E_{int} = E_{total} - (E_{MOF} + E_{NAP} + E_{water}) \quad (1)$$

where E_{int}, E_{total}, E_{MOF}, E_{NAP}, and E_{water} refer to the interaction energy, the total energy of the system, the total energy of MIL-101(Cr), the total energy of Naproxen, and the total energy of water, respectively.

In this study, we utilized the self-diffusion coefficient (D) to represnt the ability and permeation velocity of NAP molecules in MIL-101-X MOFs structures. D is determind by the Einstein Equation [51]:

$$D_i = \frac{1}{6N} \lim_{t\to\infty} \frac{d}{dt} \sum_{t=1}^{N} |r_i(t) - r_i(0)|^2 \quad (2)$$

Here $MSD = |r_i(t) - r_i(0)|^2$, N is the number of diffusing atoms, $r_i(0)$ and $r_i(t)$ are the positions of atom i between starting point and final time, respectively.

The appropriate sites for NAP adsorption in MIL-101(Cr) structures are identified by using the radial distribution function (RDF) defined as [12]:

$$g_{ij}(r) = \frac{\Delta N_{ij}(r, r+\Delta r)V}{4\pi r^2 \Delta r N_i N_j} \quad (3)$$

with r is the distance between particles i and j, $\Delta N_{ij}(r, r+\Delta r)$ as the number of particle j (NAP molecule) around i (an element of MIL-101) within a shell from r to $r+\Delta r$. N_i and N_j are the number of species i and j, and V is the system volume.

3. Results and discussion

3.1. XRD pattern characterization

Figure 4 illustrates the X-ray powder diffraction (XRD) patterns of MIL-101(Cr)-X (X = OH, F, NH_2, and SO_3H) MOFs. These MOFs exhibit the same positions for prominent peaks, observed at 2θ values of 3.3°,5°, 5.9°, 8.5°, 9°, 10.3°, and 16.6°. The positions of these peaks align closely with experimental and calculated patterns found in the literature [33, 52, 53]. Consequently, the MIL-101(Cr)-X MOFs share a similar crystal structure, but the strength of crystallinity varies, with

MIL-101(Cr)-NH_2 exhibiting the highest crystallinity. Additionally, fluorine contributes to the good crystallization of porous MOFs as noted by Jouyandeh et al.[26].

3.2. Adsorption isotherm

Adsorption capacity is an excellent standard for evaluating the adsorption of NAP pharmaculics on the surface of MOFs. Figure 5 shows the adsorption results of NAP molecules on MIL-100(Cr)-X. The amount of loading in the simulations is often high because the simulations use the pristine crystal structure of the solid, resulting a high accuracy in the adsorption isotherm of NAP on MOF [47]. Generally, MIL-101(Cr)-X MOFs exhibite a similar trend. However, functionalized MOFs with NH_2 and SO_3 have lower adsorption values compared to the pristine MOF due to a reduced pore size in the presence of functional groups. It is noted that at low pressures, adsorption of NAP molecules on the MOF surface performs rapidly because micropores are saturated quickly at low pressure, followed by the filling of mesopores. As the pressure increases, adsorption becomes slow as the occupied saturated micropores and mesopores limit the process [54].

Pre-proof

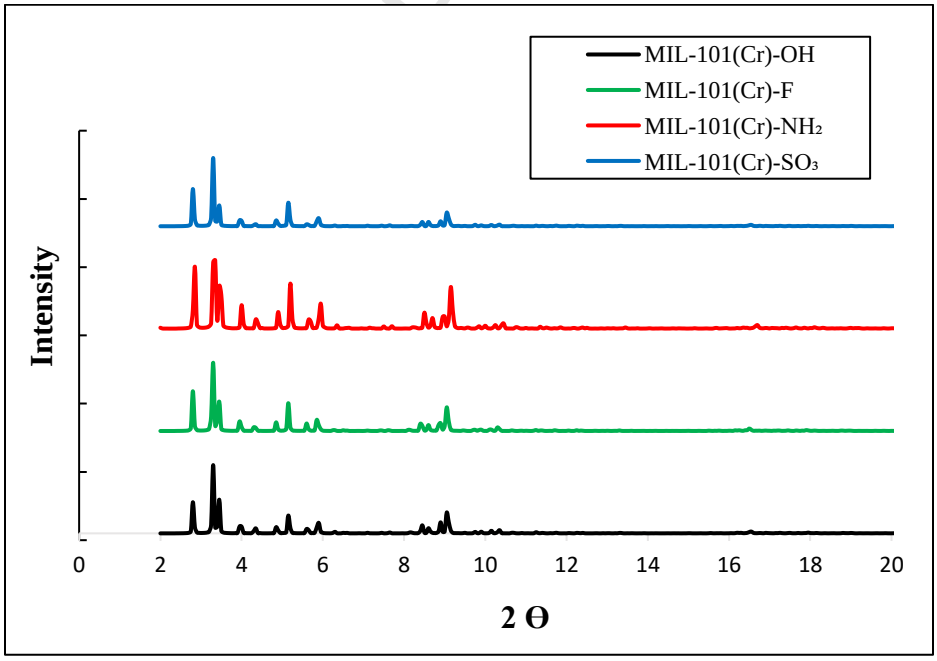

Figure 4: XRD patterns of MIL-101(Cr)-X MOFs

Table 2 compares the adsorption capacity of various adsorbents for NAP. It is evident that the adsorption capacity of NAP molecules on the MIL-101(Cr) surface are considerable, suggesting that the adsorbents are effective for removing NAP molecules from medical waste. Noticeably, it is important to note that the difference in the composition of the adsorbent materials and the experimental conditions contributes to this difference. Furthermore, MD viws the adsorbent as an ideal material, leading to achieving the highest removal capacity. Additionally, experimental and simulation studies demonstrate that the surface adsorption capacity decreases when functional active groups are added to the MIL-101(Cr) structure, as these groups impede surface adsorption.

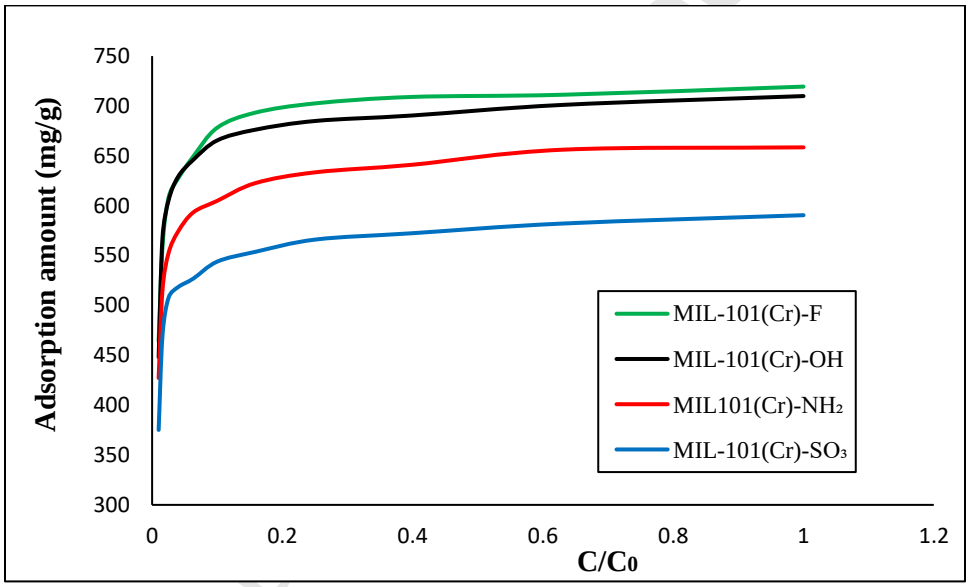

Figure 5: The NAP adsorption isotherms of MIL-101(Cr)-X

3.3. The adsorption energy

The distribution of adsorption energy for NAP molecules within the MIL-101(Cr)-OH, MIL-101(Cr)-NH2, and MIL-101(Cr)-SO3 structures is depicted in Fig. 6. The results reveal a single broad peak ranging from -25 to -45 kcal/mol that signifies the adsorption sites for NAP molecules in these MOF structures and suggests a strong attraction between NAP and solid porous structures. In contrast, the adsorption energy of NAP molecules within MIL-101(Cr)-F shows some variation. Its peak show a lower energy and higher intensity compared to the others, indicating limitations in the adsorption of NAP molecules within this structure.

Table 2: The adsorption capacity of NAP on the surface of the different adsorbents.

Adsorbents	Maximum adsorption (mg/g)	Type of work	Refs.
Cu-MIL-101-Fe	396.5	experimental	[55]
MIL-101(Cr)-$(OH)_3$	156	experimental	[28]
MIL-101(Cr)	112	experimental	[56]
MIL-101(Cr)/ GnO (3%)	171	experimental	[56]
MIL-101-SO_3	93	experimental	[33]
MIL-101-NH_2	154	experimental	[33]
MIL-101-OH	185	experimental	[57]
MIL-101-NH_2	147	experimental	[57]
MIL-53(Al)	297	experimental	[37]
CS@PANT@ZnAl-LDH composite	545.5	experimental	[6]
MIL-101(Cr)-OH	709.9	simulation	This study
MIL-101(Cr)-F	719.39	simulation	This study
MIL-101(Cr)-NH_2	658.47	simulation	This study
MIL-101(Cr)-SO_3	590.45	simulation	This study

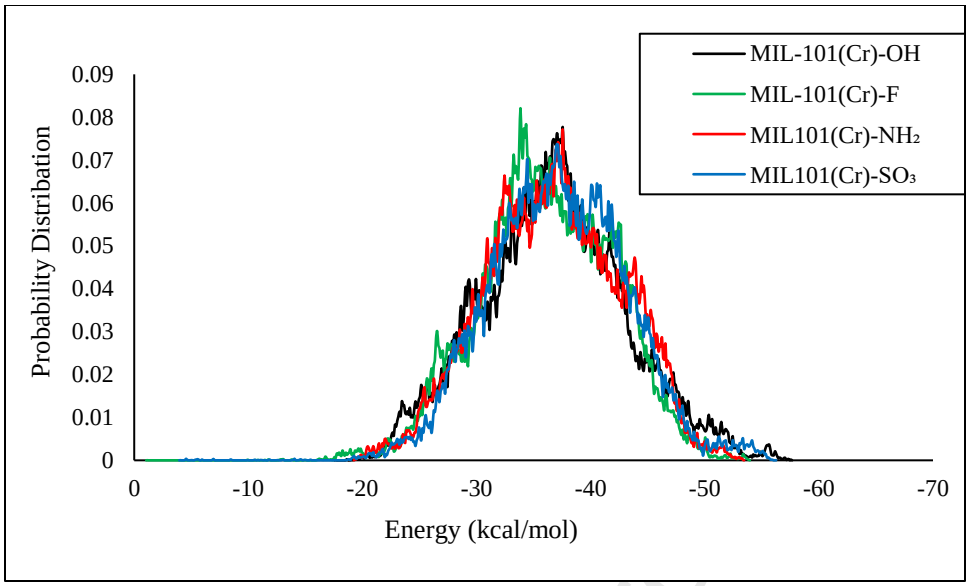

Figure 6: The adsorption energy of NAP molecules within different MOF structures.

3.4. The interaction energy between MOF and NAP

The interaction energy between MOF and NAP considers both dispersion and electrostatic contributions, and is used to describe the affinity of several adsorbates towards the adsorbent. The maximum value of the adsorption energy indicates a significant interaction between NAP molecules and the MOF surface. Figure 7 illustrates the E_{int} between NAP molecules and MIL-101(Cr)-X. It is worth noting that the presence of functional group increases the interaction energy between NAP and MIL-101(Cr)-X. Therefore, the best MOF for adsorbing NAP, based on adsorption energy, is MIL-101(Cr)-SO_3.

Journal Pre-proof

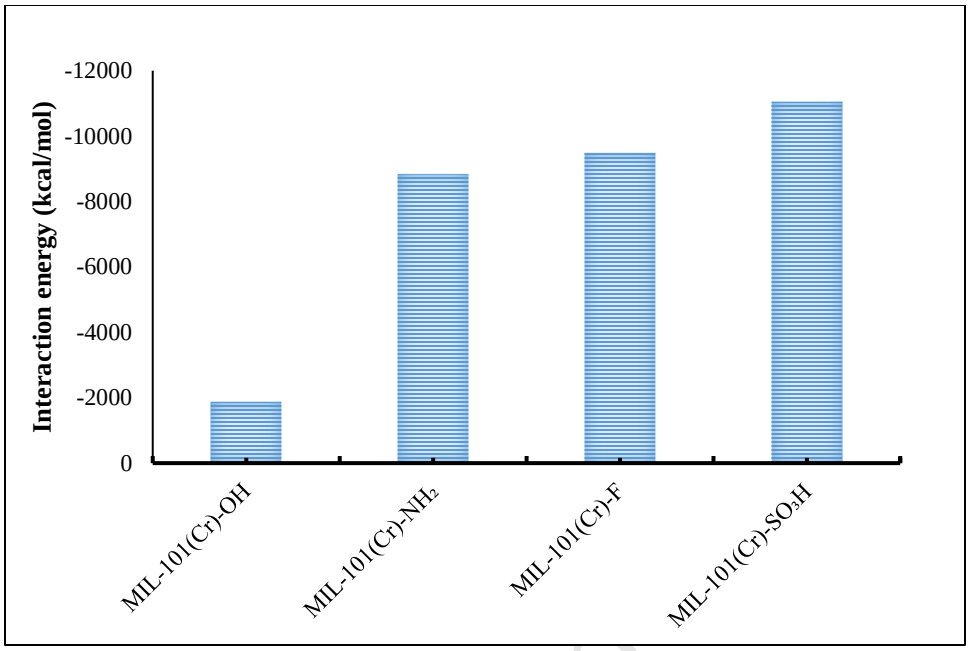

Figure 7:Interaction energy between NAP and MILs

3.5. Fractional free volume

The fractional free volume (FFV) clears molecules permeate through the membrane. A higher FFV% results in increased diffusivity for the molecules [58]. In adsorption applications, not only the minimum FFV% but also the size of the adsorbed molecule are important [51]. The simulation results of FFV for the MIL-101(Cr)-X membrane, calculated using the "Atom Volumes and Surfaces" module in the target package are shown in Fig. 8, with the corresponding FFV values listed in Table 1. When comparing the MOFs in this study, which have approximately the same density, it can be seen the smaller the FFV% of the MOF, the stronger the attraction between the MOF and Naproxen molecules. Therefore, based on the FFV% perspective, MIL-101(Cr)-SO_3 is considered the best MIL-101(Cr) for attracting Naproxen molecules. Comparing previous section demonstrates that the lowest FFV, the strongest interaction is observed.

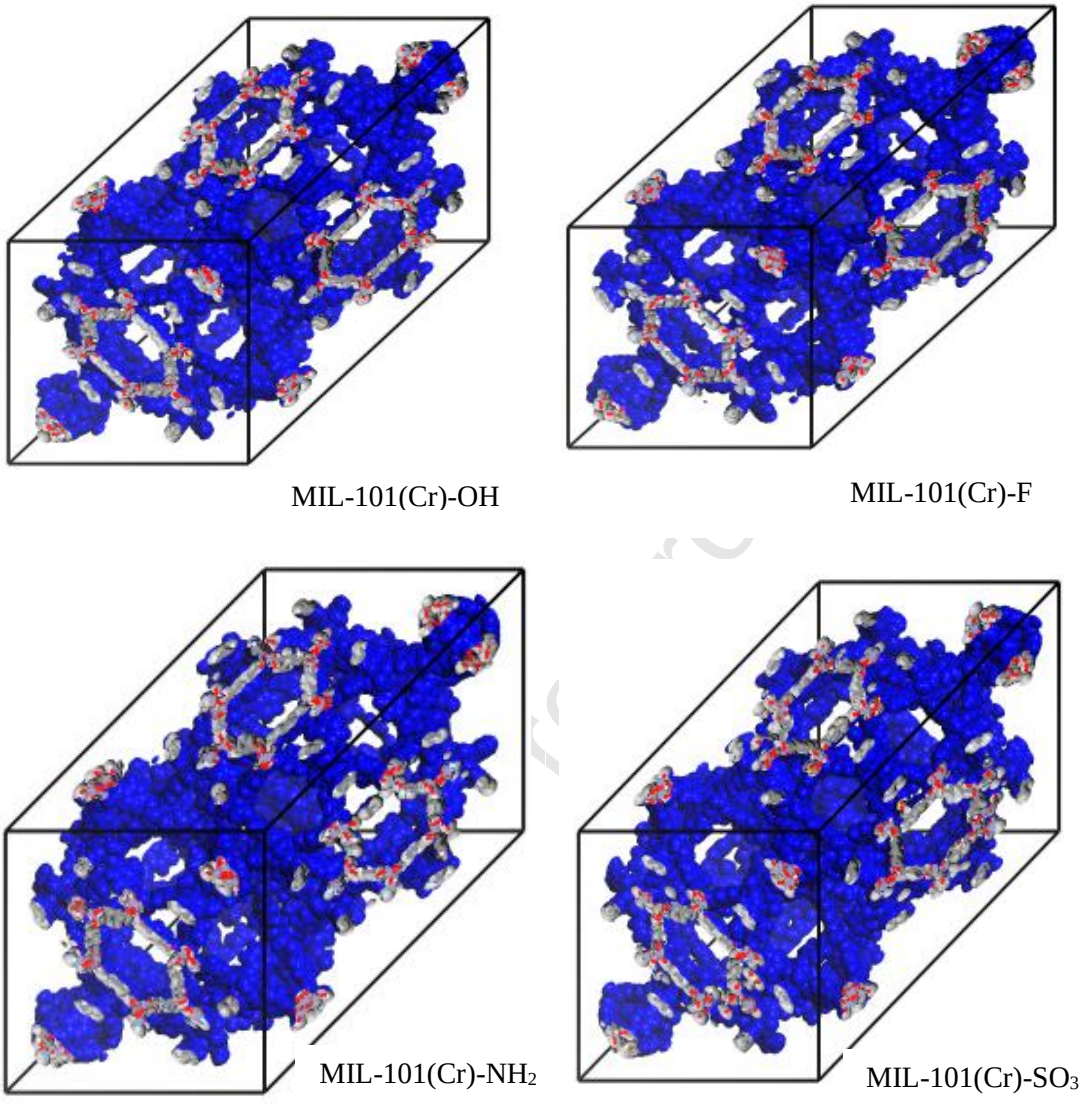

Figure 8: Simulation results of FFV of MIL-101(Cr)-X

3.6. Diffusion Coefficient

The self-diffusion coefficient is directly related to the mean rate of diffusion of NAP molecules within the structure and is calculated by determining the slope of the MSD versus simulation time. Naproxen is a large molecule involving some oxygen atoms and a benzene ring, which are highly prone to hydrogen bond and π–π stacking, respectively. Therefore, the behavior of NAP in the MIL-101(Cr)-X MOF structures may be attributed to the strong attraction of NAP molecules to the inside surface of these structures or the small size of cavities [9]. Figure 9 displays MSDs of

NAP molecules in different MIL-101(Cr)-X MOFs versas time. The results indicate that the least MSD of NAP molecules occurres in MIL-101(Cr)-SO_3. In other word, the lowest freedom to move inside the adsorbent that is in accordance with greatest interation energy.

Considering the structural properties of the MIL-101(Cr)-X structures in Table 1, MIL-101(Cr)-SO_3, with the highest specific surface area and lowest FFV does not readily allow NAP molecules to diffuse easily. However, MIL-101(Cr)-NH_2, with a density and FFV of 0.487 g/cm^3 and 81.29%, respectively, has suitable porosity and cavity size, making it conducive to permeate NAP. The low MSD of NAP molecules in the MOF is due to the strong interactions between the NAP molecules and MIL-101(Cr)-SO_3 atoms while MIL-101(OH) and MIL-101(F) exhibit almost the same MSD with similar FFV% and adsorption capacities.

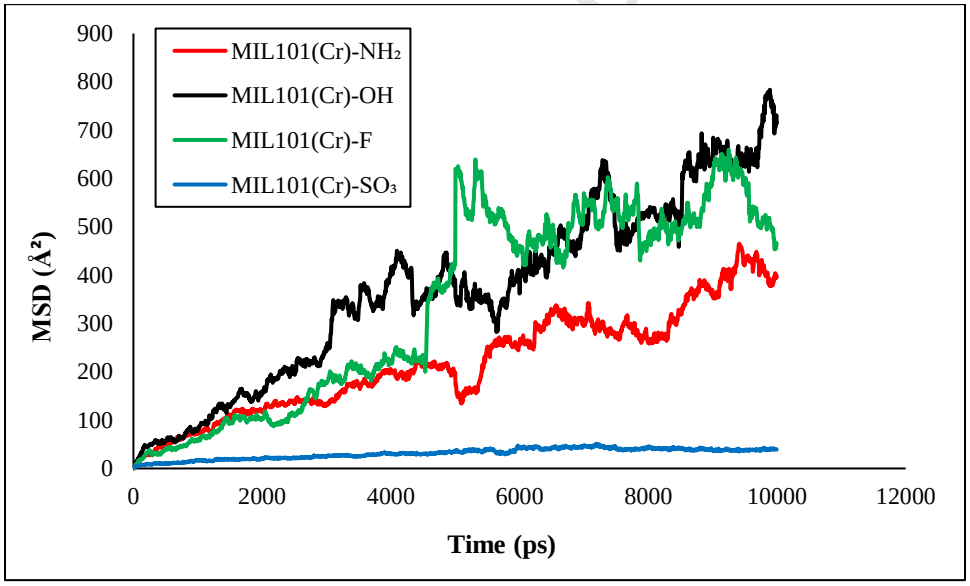

Figure 9: MSD of NAP molecules in the different MIL-101 structures

Figure 10 illustrates the impact of MOFs' porosity on the diffusion coefficient by demonstrating the correlation between the diffusion coefficient of NAP molecules and FFV%. The observations indicate that as the FFV% of the MIL-101(Cr) structure increases, signifying higher porosity, the diffusion coefficient of NAP molecules also increases. Specifically, the results depicted in Figure 10 reveal that when active functional groups are present, MIL-101(Cr)-SO_3 outperforms MIL-101(Cr)-NH_2 in capturing NAP molecules and effectively removing them from the solution.

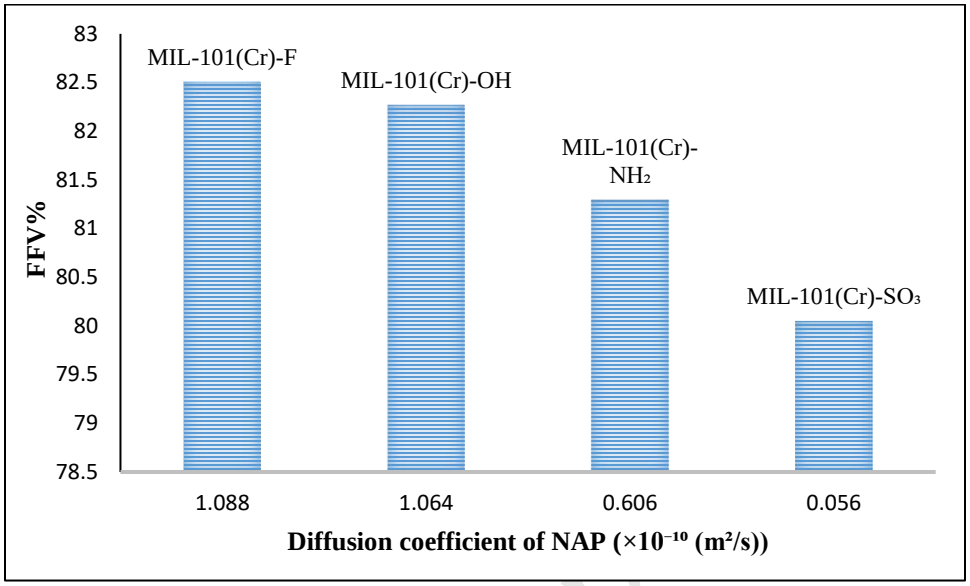

Figure 10: The diffusion coefficient NAP in the different MOF structures versus FFV%.

Table 3 compares the adsorption capacity and diffusion coefficient of various materials in the MIL-101(Cr) adsorbent. It is important to note that both properties MIL-101(Cr) depend on the size of the sorbent, its composition, and its active functional groups containment. Specifically, the absorption capacity of NAP in MIL-101(Cr) is lower compared to other adsorbed substances due to the large size of the Naproxen molecule.

Table 3: The adsorption capacity and diffusion coefficient of different materials in MIL-101(Cr)

Structures	**Specific surface area (m^2/g)**	**Adsorption capacity (mg/g)**	**× 10^{-10} (m^2/s) diffusion**	**Refs.**
Terephthalic acid	3284.80	1585.02	12.100	[9]
water	3298.00	1440.00	0.670	[39]
Ethyl Acetate	3446.00	880.00	1.927	[59]

Benzene	3054.00	1171.56	0.004	[60]
Toluene	3368.00	397.69	0.294	[61]
Naproxen	3918.84	553.05	1.064	This study

3.7. The affinity between NAP molecules and different atoms of MIL-101(Cr)s

The radial distribution function (RDF) shed lights on the adsorption sites. RDFs between NAP molecules and different atoms of MIL-101(Cr) were calculated for this purpose. Figure 11 displays the RDFs of NAP molecules around Cr, O, C, F, S, and N atoms of MIL-101(Cr)-X. For all the target MOFs, a sharp peak between 0.37 nm and 1 nm was observed in Figure 11a that indicates the surface potential shown by the unsaturated positions of Cr atoms has a strong affinity for NAP molecules. Additionally, MIL-101(Cr)-SO_3 has a peak located at 0.52 nm, suggesting that NAP molecules bind to Cr atoms according to Lewis' rule due to the sturdy quadrupole moment.

In Figure 11b, for MIL-101(Cr)-OH, MIL-101(Cr)-F, and MIL-101(Cr)-NH_2 a slightly broad peak (between 0.3 nm and 1.1 nm) is observed, indicating an affinity between NAP molecules and the oxygen atoms of these MOFs, although weaker than with chromium atoms. A broader peak (between 0.3 nm and 1.4 nm) is seen for MIL-101(Cr)-SO_3, suggesting a weaker affinity due to the hindrance caused by the large size of the sulfonic group (SO_3).

Figure 11c shows the attraction between Naproxen molecules and carbon atoms of the MIL-101(Cr). A broad peak between 0.5 nm and 1.5 nm is observed for all MIL-101(Cr)-X solids, indicating a weak affinity between NAP molecules and carbon atoms. In Figure 11d, sharp peaks at 2.15 Å are seen for both MIL-101(Cr)-F and MIL-101(Cr)-NH_2, indicating a strong interaction and preference for adsorption on these MOFs. The peak for MIL-101(Cr)-F is stronger, suggesting greater adsorption capacity and interaction energy compared to MIL-101(Cr)-NH_2.

Aside from oxygen, carbon, and chromium atoms, sulfur atom in MIL-101(Cr)-SO_3 and nitrogen atom in MIL-101(Cr)-NH_2 also attract NAP molecules. The RDF of NAP-S (Figure 11e) and NAP-N (Figure 11f) show a first peak with high intensity located at 4.25 Å and 2.49 Å, respectively. This indicates that MIL-101(Cr)-NH_2 has a greater adsorption capacity than MIL-101(Cr)-SO_3, consistent with the results of MSD and adsorption isotherm. However, MIL-101(Cr)-SO_3 has a strong peak at 4.25 Å, indicating greater interaction energy with NAP molecules compared to MIL-101(Cr)-NH_2, likely due to acid-base interaction between the SO_3 group and naproxen molecules.

4- Conclusion

In this study, molecular dynamic simulation was carried out to investigate the adsorption properties of Naproxen molecules on MIL-101(Cr)-X and the effect of activated functional groups including OH, F, NH_2 and SO_3 on Naproxen adsorption was under investigation. The molecular dynamics study considers the adsorbent as an ideal material, allowing for a detailed description of the adsorption process. The simulation results indicate that the lower fractional free volume of MIL-101(Cr) led to porosity, resulting in a higher removal capacity of NAP from aqueous solution. The RDF results demonstrate that Naproxen molecules energetically preferred to be adsorbed on MIL-101(Cr)-SO_3 and MIL-101(Cr)-NH_2 due to strong interactions between S and N atoms in these MOFs and Naproxen molecules. Additionally, Naproxen molecules exhibit Lewis rule-bound behavior with Cr atoms, attributed to a sturdy quadrupole moment. MIL-101(Cr) showed promising results in attracting and removing Naproxen, suggesting potential for improved efficiency by combining MIL-101(Cr)-X with other formulations such as polymers, carbon nanotubes, graphene oxide, ete.

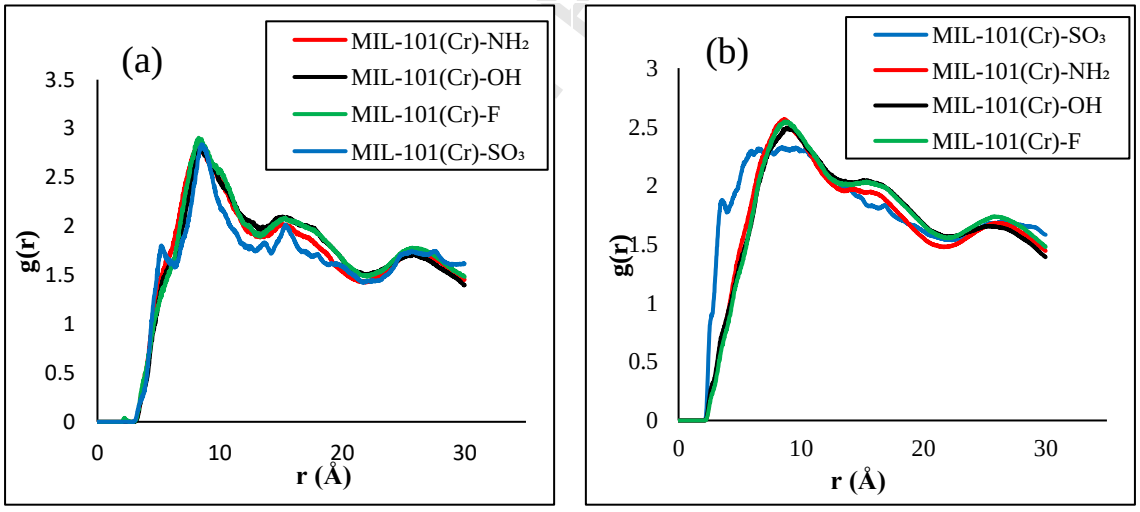

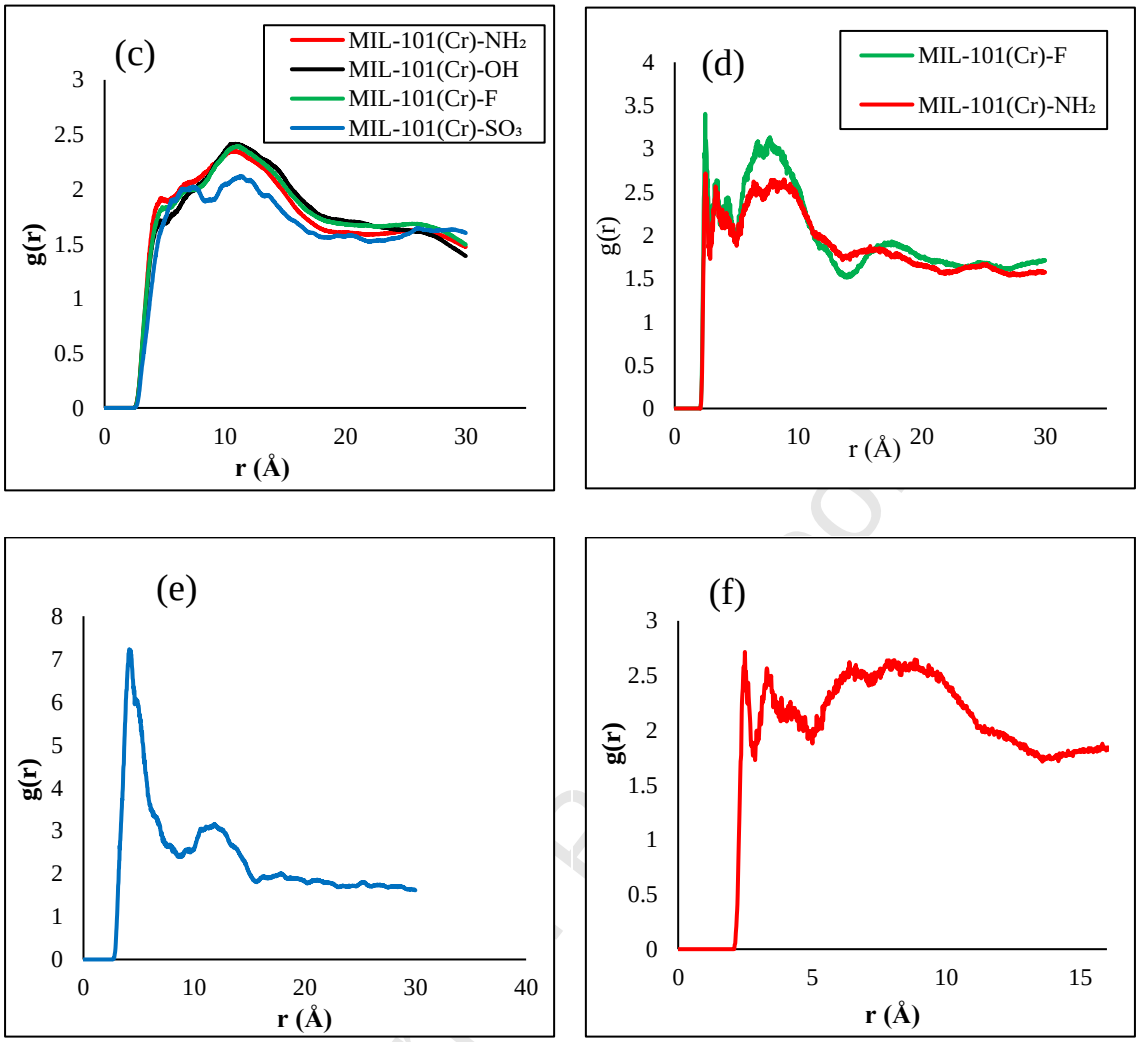

Figure 11*:* Radial distribution function of (a): NAP-Cr (b): NAP-O (c): NAP-C (d): NAP-F (e): NAP-S in MIL-101(Cr)-SO_3 and (f): NAP-N in MIL-101(Cr)-NH_2.

Declaration of Interests

The authors declare that they have no known competing financial interests or personal relationships that could have influenced the work reported in this paper.

Acknowledgments

The authors would like to thank Ferdowsi University of Mashhad (FUM) for providing computational support for this research.

References:

[1] S. Bindu, S. Mazumder, U. Bandyopadhyay, Non-steroidal anti-inflammatory drugs (NSAIDs) and organ damage: A current perspective, Biochemical pharmacology, 180 (2020) 114147.
[2] R.S. Wong, Role of nonsteroidal anti-inflammatory drugs (NSAIDs) in cancer prevention and cancer promotion, Advances in pharmacological sciences, 2019 (2019).
[3] A. Rastogi, M.K. Tiwari, M.M. Ghangrekar, A review on environmental occurrence, toxicity and microbial degradation of Non-Steroidal Anti-Inflammatory Drugs (NSAIDs), Journal of Environmental Management, 300 (2021) 113694.
[4] E. Tyumina, G. Bazhutin, A.d.P. Cartagena Gómez, I. Ivshina, Nonsteroidal anti-inflammatory drugs as emerging contaminants, Microbiology, 89 (2020) 148-163.
[5] L. Xing, K.M. Haddao, N. Emami, F. Nalchifard, W. Hussain, A.H. Dawood, D. Toghraie, M. Hekmatifar, Fabrication of HKUST-1/ZnO/SA nanocomposite for Doxycycline and Naproxen adsorption from contaminated water, Sustainable Chemistry and Pharmacy, 29 (2022) 100757.
[6] H. Xu, S. Zhu, M. Xia, F. Wang, X. Ju, Three-dimension hierarchical composite via in-situ growth of Zn/Al layered double hydroxide plates onto polyaniline-wrapped carbon sphere for efficient naproxen removal, Journal of Hazardous Materials, 423 (2022) 127192.
[7] W. Sun, H. Li, H. Li, S. Li, X. Cao, Adsorption mechanisms of ibuprofen and naproxen to UiO-66 and UiO-66-NH2: Batch experiment and DFT calculation, Chemical Engineering Journal, 360 (2019) 645-653.
[8] S. Aydin, M.E. Aydin, A. Ulvi, Monitoring the release of anti-inflammatory and analgesic pharmaceuticals in the receiving environment, Environmental Science and Pollution Research, 26 (2019) 36887-36902.
[9] A. Bigdeli, F. Khorasheh, S. Tourani, A. Khoshgard, H.H. Bidaroni, Molecular simulation study of the adsorption and diffusion properties of terephthalic acid in various metal organic frameworks, Journal of Inorganic and Organometallic Polymers and Materials, 30 (2020) 1643-1652.
[10] K.A. Adegoke, O.S. Agboola, J. Ogunmodede, A.O. Araoye, O.S. Bello, Metal-organic frameworks as adsorbents for sequestering organic pollutants from wastewater, Materials Chemistry and Physics, 253 (2020) 123246.
[11] R. Pelalak, R. Soltani, Z. Heidari, R.E. Malekshah, M. Aallaei, A. Marjani, M. Rezakazemi, T.A. Kurniawan, S. Shirazian, Molecular dynamics simulation of novel diamino-functionalized hollow mesosilica spheres for adsorption of dyes from synthetic wastewater, Journal of Molecular Liquids, 322 (2021) 114812.
[12] M. Wehbe, B.J.A. Tarboush, M. Shehadeh, M. Ahmad, Molecular dynamics simulations of the removal of lead (II) from water using the UiO-66 metal-organic framework, Chemical Engineering Science, 214 (2020) 115396.
[13] J. Lach, A. Szymonik, Adsorption of naproxen sodium from aqueous solutions on commercial activated carbons, Journal of Ecological Engineering, 20 (2019).
[14] D.S. Franco, J. Georgin, M.S. Netto, K. da Boit Martinello, L.F. Silva, Preparation of activated carbons from fruit residues for the removal of naproxen (NPX): Analytical interpretation via statistical physical model, Journal of Molecular Liquids, 356 (2022) 119021.
[15] Y. Cao, A. Khan, F. Ghorbani, H. Mirzaei, P. Singla, H. Balakheyli, A. Soltani, M. Aghaei, Z. Azmoodeh, M. Aarabi, Predicting adsorption behavior and anti-inflammatory activity of naproxen interacting with pure boron nitride and boron phosphide fullerene-like cages, Journal of Molecular Liquids, 339 (2021) 116678.
[16] K. Jedynak, B. Szczepanik, N. Rędzia, P. Słomkiewicz, A. Kolbus, P. Rogala, Ordered mesoporous carbons for adsorption of paracetamol and non-steroidal anti-inflammatory drugs: ibuprofen and naproxen from aqueous solutions, Water, 11 (2019) 1099.
[17] D. Smiljanić, B. de Gennaro, A. Daković, B. Galzerano, C. Germinario, F. Izzo, G.E. Rottinghaus, A. Langella, Removal of non-steroidal anti-inflammatory drugs from water by zeolite-rich composites: The

Journal Pre-proof

interference of inorganic anions on the ibuprofen and naproxen adsorption, Journal of Environmental Management, 286 (2021) 112168.
[18] B. Czech, M. Kończak, M. Rakowska, P. Oleszczuk, Engineered biochars from organic wastes for the adsorption of diclofenac, naproxen and triclosan from water systems, Journal of Cleaner Production, 288 (2021) 125686.
[19] M. Safaei, M.M. Foroughi, N. Ebrahimpoor, S. Jahani, A. Omidi, M. Khatami, A review on metal-organic frameworks: Synthesis and applications, TrAC Trends in Analytical Chemistry, 118 (2019) 401-425.
[20] Y.-y. Zhao, Y.-l. Liu, X.-m. Wang, X. Huang, Y.F. Xie, Impacts of metal–organic frameworks on structure and performance of polyamide thin-film nanocomposite membranes, ACS applied materials & interfaces, 11 (2019) 13724-13734.
[21] A. Bateni, I. Salahshoori, M.N. Jorabchi, M.M. Mohseni, M.R. Asadabadi, H.A. Khonakdar, Molecular simulation-based assessing of a novel metal-organic framework modified with alginate and chitosan biopolymers for anionic reactive black 5 and cationic crystal violet pollutants capture, Separation and Purification Technology, 354 (2025) 128986.
[22] R. Miladi, I. Salahshoori, M. Golriz, M. Raji, A. Ranjbarzadeh-Dibazar, G. Naderi, H.A. Khonakdar, Computational insights into pectin and chitosan-enhanced MOFs: A green pathway for pollutant remediation, Process Safety and Environmental Protection, 192 (2024) 862-877.
[23] I. Salahshoori, M.N. Jorabchi, S. Ghasemi, A. Ranjbarzadeh-Dibazar, M. Vahedi, H.A. Khonakdar, MIL-53 (Al) nanostructure for non-steroidal anti-inflammatory drug adsorption in wastewater treatment: Molecular simulation and experimental insights, Process Safety and Environmental Protection, 175 (2023) 473-494.
[24] I. Salahshoori, A. Vaziri, R. Jahanmardi, M.M. Mohseni, H.A. Khonakdar, Molecular simulation studies of pharmaceutical pollutant removal (rosuvastatin and simvastatin) using novel modified-MOF nanostructures (UIO-66, UIO-66/chitosan, and UIO-66/oxidized chitosan), ACS Applied Materials & Interfaces, 16 (2024) 26685-26712.
[25] S. Rojas, P. Horcajada, Metal–organic frameworks for the removal of emerging organic contaminants in water, Chemical reviews, 120 (2020) 8378-8415.
[26] M. Jouyandeh, F. Tikhani, M. Shabanian, F. Movahedi, S. Moghari, V. Akbari, X. Gabrion, P. Laheurte, H. Vahabi, M.R. Saeb, Synthesis, characterization, and high potential of 3D metal–organic framework (MOF) nanoparticles for curing with epoxy, Journal of Alloys and Compounds, 829 (2020) 154547.
[27] S. Karmakar, D. Roy, C. Janiak, S. De, Insights into multi-component adsorption of reactive dyes on MIL-101-Cr metal organic framework: Experimental and modeling approach, Separation and Purification Technology, 215 (2019) 259-275.
[28] J.Y. Song, S.H. Jhung, Adsorption of pharmaceuticals and personal care products over metal-organic frameworks functionalized with hydroxyl groups: quantitative analyses of H-bonding in adsorption, Chemical Engineering Journal, 322 (2017) 366-374.
[29] J.M. Park, S.H. Jhung, A remarkable adsorbent for removal of bisphenol S from water: aminated metal-organic framework, MIL-101-NH2, Chemical Engineering Journal, 396 (2020) 125224.
[30] F. Aouaini, N. Bouaziz, N. Khemiri, H. Alyoussef, S. Nasr, A. Ben Lamine, Adsorption of methyl orange, acid chrome blue K, and Congo red dyes on MIL-101-NH2 adsorbent: Analytical interpretation via advanced model, AIP advances, 12 (2022) 035307.
[31] H. Jalayeri, P. Aprea, D. Caputo, A. Peluso, F. Pepe, Synthesis of amino-functionalized MIL-101 (Cr) MOF for hexavalent chromium adsorption from aqueous solutions, Environmental nanotechnology, monitoring & management, 14 (2020) 100300.
[32] I. Salahshoori, M.N. Jorabchi, S.M.S. Mirnezami, M. Golriz, M. Darestani, J. Barzin, H.A. Khonakdar, Exploring the potential of beta-cyclodextrin-based MIL-101 (Cr) for pharmaceutical removal from wastewater: A combined density functional theory and molecular simulations study, Environmental Research, 263 (2024) 120189.

[33] Z. Hasan, E.-J. Choi, S.H. Jhung, Adsorption of naproxen and clofibric acid over a metal–organic framework MIL-101 functionalized with acidic and basic groups, Chemical engineering journal, 219 (2013) 537-544.
[34] N. Prasetya, I.G. Wenten, M. Franzreb, C. Wöll, Metal-organic frameworks for the adsorptive removal of pharmaceutically active compounds (PhACs): comparison to activated carbon, Coordination Chemistry Reviews, 475 (2023) 214877.
[35] A.A. Castañeda Ramírez, E. Rojas García, R. López Medina, J.L. Contreras Larios, R. Suárez Parra, A.M. Maubert Franco, Selective adsorption of aqueous diclofenac sodium, naproxen sodium, and ibuprofen using a stable FE3O4–FEBTC metal–organic framework, Materials, 14 (2021) 2293.
[36] M. Cheraghian, H. Alinezhad, S. Ghasemi, M. Moalem-Banhangi, Modified Metal-Organic Frameworks as an Efficient Nanoporous Adsorbent for the Removal of Naproxen from Water Sources, Polycyclic Aromatic Compounds, 43 (2022) 1-14.
[37] A. Karami, R. Sabouni, M. Ghommem, Experimental investigation of competitive co-adsorption of naproxen and diclofenac from water by an aluminum-based metal-organic framework, Journal of Molecular Liquids, 305 (2020) 112808.
[38] G. Pena-Velasco, L. Hinojosa-Reyes, A. Hernandez-Ramirez, L. Sandoval-Rangel, J.L. Guzmán-Mar, Enhanced Removal of Low Concentrations of Anti-inflammatory Drugs in Water Using Fe-MOF Derived Carbon Treated by Acidic Leaching: Characterization and Performance, Journal of Inorganic and Organometallic Polymers and Materials, 32 (2022) 4204-4215.
[39] S. Fei, A. Alizadeh, W.-L. Hsu, J.-J. Delaunay, H. Daiguji, Analysis of the water adsorption mechanism in metal–organic framework MIL-101 (Cr) by molecular simulations, The Journal of Physical Chemistry C, 125 (2021) 26755-26769.
[40] N. Montazeri, I. Salahshoori, P. Feyzishendi, F.S. Miri, M.M. Mohseni, H.A. Khonakdar, pH-Sensitive adsorption of gastrointestinal drugs (famotidine and pantoprazole) as pharmaceutical pollutants by using the Au-doped@ ZIF-90-glycerol adsorbent: insights from computational modeling, Journal of Materials Chemistry A, 11 (2023) 26127-26151.
[41] I. Salahshoori, N. Montazeri, A. Yazdanbakhsh, M. Golriz, R. Farhadniya, H.A. Khonakdar, Insights into the adsorption properties of mixed matrix membranes (Pebax 1657-g-Chitosan-PVDF-Bovine Serum Albumin@ ZIF-CO3-1) for the Antiviral COVID-19 treatment drugs remdesivir and nirmatrelvir: An in silico study, ACS Applied Materials & Interfaces, 15 (2023) 31185-31205.
[42] I. Salahshoori, M.A. Nobre, A. Yazdanbakhsh, R.E. Malekshah, M. Asghari, H.A. Khonakdar, A.H. Mohammadi, Navigating the molecular landscape of environmental science and heavy metal removal: A simulation-based approach, Journal of Molecular Liquids, 410 (2024) 125592.
[43] A. Mohmmad, M.H. Mosavian, F. Moosavi, Pharmaceutically active compounds removal from aqueous solutions by MIL-101 (Cr)-NH2: A molecular dynamics study, Ecotoxicology and Environmental Safety, 278 (2024) 116333.
[44] A. Mohmmad, M.H. Mosavian, F. Moosavi, Investigation of Polyphenylene sulfide polymer in removing drug molecules from solution using molecular dynamics simulations, Materials Chemistry and Physics, 340 (2025) 130773.
[45] I. Salahshoori, M.N. Jorabchi, A. Mazaheri, S.M.S. Mirnezami, M. Afshar, M. Golriz, M.A. Nobre, Tackling antibiotic contaminations in wastewater with novel Modified-MOF nanostructures: A study of molecular simulations and DFT calculations, Environmental Research, 252 (2024) 118856.
[46] D. Feng, Y. Feng, Y. Zang, P. Li, X. Zhang, Phase change in modified metal organic frameworks MIL-101 (Cr): Mechanism on highly improved energy storage performance, Microporous and Mesoporous Materials, 280 (2019) 124-132.
[47] M.F. De Lange, J.-J. Gutierrez-Sevillano, S. Hamad, T.J. Vlugt, S. Calero, J. Gascon, F. Kapteijn, Understanding adsorption of highly polar vapors on mesoporous MIL-100 (Cr) and MIL-101 (Cr): Experiments and molecular simulations, The Journal of Physical Chemistry C, 117 (2013) 7613-7622.

[48] K. Zhang, Y. Chen, A. Nalaparaju, J. Jiang, Functionalized metal–organic framework MIL-101 for CO 2 capture: multi-scale modeling from ab initio calculation and molecular simulation to breakthrough prediction, CrystEngComm, 15 (2013) 10358-10366.
[49] M. Ayvaz Koroglu, O. Kurkcuoglu, F.A. Sungur, Monte Carlo and Molecular Dynamics Simulations suggest controlled release of corticosteroids from mesoporous host MIL-101 (Cr), Molecular Simulation, 47 (2021) 1530-1539.
[50] X. Huang, J. Lu, W. Wang, X. Wei, J. Ding, Experimental and computational investigation of CO2 capture on amine grafted metal-organic framework NH2-MIL-101, Applied Surface Science, 371 (2016) 307-313.
[51] I. Salahshoori, A. Seyfaee, A. Babapoor, F. Neville, R. Moreno-Atanasio, Evaluation of the effect of silica nanoparticles, temperature and pressure on the performance of PSF/PEG/SiO2 mixed matrix membranes: A molecular dynamics simulation (MD) and design of experiments (DOE) study, Journal of Molecular Liquids, 333 (2021) 115957.
[52] E. Gkaniatsou, R. Ricoux, K. Kariyawasam, I. Stenger, B. Fan, N. Ayoub, S. Salas, G. Patriarche, C. Serre, J.-P. Mahy, Encapsulation of microperoxidase-8 in MIL-101 (Cr)-X nanoparticles: influence of metal–organic framework functionalization on enzymatic immobilization and catalytic activity, ACS Applied Nano Materials, 3 (2020) 3233-3243.
[53] C. Song, R. Li, Z. Fan, Q. Liu, B. Zhang, Y. Kitamura, CO2/N2 separation performance of Pebax/MIL-101 and Pebax/NH2-MIL-101 mixed matrix membranes and intensification via sub-ambient operation, Separation and Purification Technology, 238 (2020) 116500.
[54] G. Hu, W. Li, S. Li, Effects of functionalization on the performance of metal-organic frameworks for adsorption-driven heat pumps by molecular simulations, Chemical Engineering Science, 208 (2019) 115143.
[55] P. Xiong, H. Zhang, G. Li, C. Liao, G. Jiang, Adsorption removal of ibuprofen and naproxen from aqueous solution with Cu-doped Mil-101 (Fe), Science of The Total Environment, 797 (2021) 149179.
[56] M. Sarker, J.Y. Song, S.H. Jhung, Adsorptive removal of anti-inflammatory drugs from water using graphene oxide/metal-organic framework composites, Chemical Engineering Journal, 335 (2018) 74-81.
[57] P.W. Seo, B.N. Bhadra, I. Ahmed, N.A. Khan, S.H. Jhung, Adsorptive removal of pharmaceuticals and personal care products from water with functionalized metal-organic frameworks: remarkable adsorbents with hydrogen-bonding abilities, Scientific reports, 6 (2016) 1-11.
[58] K. Golzar, H. Modarress, S. Amjad-Iranagh, Separation of gases by using pristine, composite and nanocomposite polymeric membranes: A molecular dynamics simulation study, Journal of Membrane Science, 539 (2017) 238-256.
[59] J. Shi, Z. Zhao, Q. Xia, Y. Li, Z. Li, Adsorption and diffusion of ethyl acetate on the chromium-based metal–organic framework MIL-101, Journal of Chemical & Engineering Data, 56 (2011) 3419-3425.
[60] Z. Zhao, X. Li, S. Huang, Q. Xia, Z. Li, Adsorption and diffusion of benzene on chromium-based metal organic framework MIL-101 synthesized by microwave irradiation, Industrial & Engineering Chemistry Research, 50 (2011) 2254-2261.
[61] J. Wang, Y. Muhammad, Z. Gao, S.J. Shah, S. Nie, L. Kuang, Z. Zhao, Z. Qiao, Z. Zhao, Implanting polyethylene glycol into MIL-101 (Cr) as hydrophobic barrier for enhancing toluene adsorption under highly humid environment, Chemical Engineering Journal, 404 (2021) 126562.

Journal Pre-proof

Declaration of interests

☐ The authors declare that they have no known competing financial interests or personal relationships that could have appeared to influence the work reported in this paper.

☒The authors declare the following financial interests/personal relationships which may be considered as potential competing interests:

Ferdowsi University of Mashhad (Iran)

Journal Pre-proof

Graphical abstract

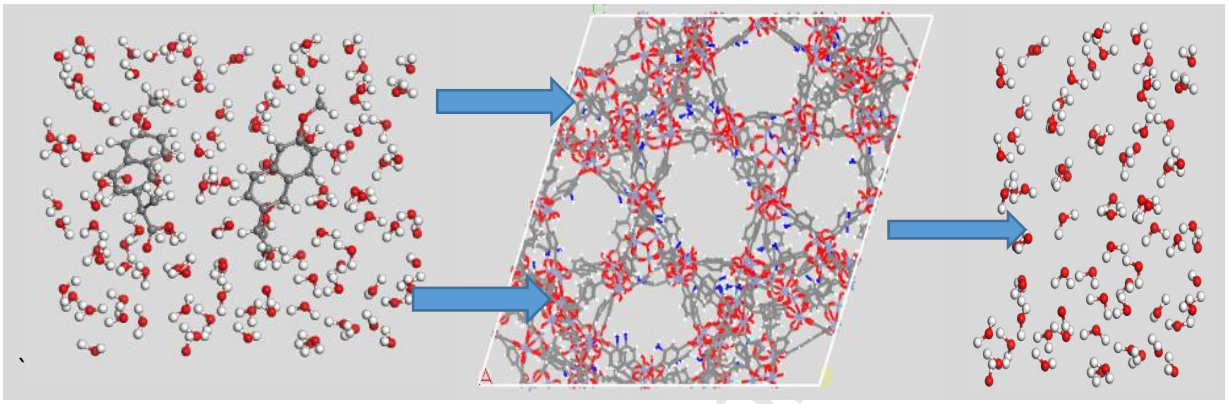

Journal Pre-proof